Journal of Biomechanics 42 (2009) 1850–1855

Contents lists available at ScienceDirect

Journal of Biomechanics

journal homepage: www.elsevier.com/locate/jbiomech
www.JBiomech.com

Evaluation of the roles of passive and active control of balance using a balance control model

Xingda Qu [a,*], Maury A. Nussbaum [b,1]

[a] School of Mechanical and Aerospace Engineering, Nanyang Technological University, Singapore 639798, Singapore
[b] Department of Industrial and Systems Engineering, Virginia Tech 250 Durham Hall (0118), Blacksburg, VA 24061, USA

ARTICLE INFO

Article history:
Accepted 17 May 2009

Keywords:
Balance
Postural control
Active/passive control
Center of pressure

ABSTRACT

At present there is a lack of consensus regarding the relative roles of passive and active control of quiet upright stance. In the current work, this issue was investigated using two simulation models based on contemporary theories. Specifically, the two models, both of which assumed active control torques to be generated from an optimal neural controller, differed with respect to whether or not passive control torques (stiffness and damping) were included. Model parameters were specified using experimental center-of-pressure (COP) time series obtained during upright stance, and comparisons then made between simulated and actual COP-based measures. Including both active and passive joint torques in the control model did not appear to lead to any improvement in the ability to simulate COP compared with only including active joint torque. Further, simulated passive control torques were typically less than 10% of the active control torques, though some exceptions were found. These results, along with existing empirical evidence, suggest that active control torque is dominant in maintaining balance during upright stance.

1. Introduction

Human upright posture is inherently unstable and is maintained by control torques generated from the postural control system. Recently, the relative roles or importance of passive and active control torques in balance control has been an object of discussion and controversy (e.g., Morasso and Schieppati, 1999; Winter et al., 2001). Passive control torques are considered to stem from intrinsic tissue mechanical properties (i.e., stiffness or damping), and to act without time delay (e.g., Winter et al., 1998, 2001). In contrast, active control torques are generated by active muscle contraction regulated by the neural controller (e.g., Applegate et al., 1988).

Some studies (e.g., Winter et al., 1998, 2001, 2003) have suggested that passive control is the major means by which the postural control system maintains balance in the context of controlling quiet upright stance. For example, Winter et al. (2001) directly estimated muscle stiffness from ankle joint torque and sway angle; a high correspondence between ankle torque and sway angle indicated that ankle stiffness approached an ideal spring and was the controlling element in postural sway. In contrast, some studies (e.g., Morasso and Sanguineti, 2002; Morasso and Schieppati, 1999; Loram and Lakie, 2002a, 2002b; Lakie et al., 2003) have suggested that passive torque alone is not sufficient to stabilize the body as an inverted pendulum, and that additional active torque regulated by the neural controller is necessary. For example, Casadio et al. (2005) measured intrinsic ankle stiffness directly, and then compared it with the critical stiffness, the latter being the minimal necessary to achieve stability without an active stabilization mechanism. They reported that intrinsic ankle stiffness during quiet standing was only 64±8% of the critical stiffness, and concluded that active neural control is necessary.

Identifying the roles of passive and active control torques in balance control can lead to a better understanding of balance control mechanisms, and further aid in the improvement and/or maintenance of balance (e.g., to counteract the adverse effects of aging or neurological disorders). As yet, no consensus regarding these roles has been reached, and the purpose of this study was to provide additional evidence from a different perspective. The basis for the present investigation is a recently developed balance control model of quiet upright stance. Unlike other balance control models, this model assumes that human motions are optimized – an assumption which is reasonable according to previous evidence (e.g., Ohta et al., 2004; Fagg et al., 2002) – and this model appears to generate realistic simulations of measures

* Corresponding author. Tel.: +65 67904458; fax: +65 67924062.
E-mail addresses: xdqu@ntu.edu.sg (X. Qu), nussbaum@vt.edu (M.A. Nussbaum)
[1] Tel.: +1 540 231 6053; fax: +1 540 231 3322.

0021-9290/$ - see front matter © 2009 Elsevier Ltd. All rights reserved.
doi:10.1016/j.jbiomech.2009.05.036

derived from center-of-pressure (COP) time series under several conditions (Qu et al., 2007; Qu and Nussbaum, 2009). Specifically, we used this balance control model to evaluate the relative roles of passive and active control of balance using two alternative model structures. Several previous studies have adopted only active control torque in balance control models, yet could simulate reasonable sway behaviors (e.g., Masani et al., 2006; Maurer and Peterka, 2005). Based on this, we hypothesized that active control torque would be relatively important in balance control.

2. Methods

2.1. Participants and experimental procedures

Experimental data were required to specify model parameters (as summarized below). Eight male and eight female participants (18–24 years) without self-reported injuries, illness, or musculoskeletal disorders were included in the study. During experimental trials, the participants stood upright on a force platform (AMTI OR6-7-1000, Watertown, Massachusetts, USA) as still as possible with their eyes closed. Each trial was 75 s in duration, and the initial 10 s and last 5 s were removed. Participants performed three trials, with at least 1 min of rest between each. Triaxial ground reaction forces and moments collected by the force platform were sampled at 100 Hz, low-pass filtered (5 Hz cut-off, 2nd order, Butterworth) in software, and subsequently used to derive COP time series.

The model-based simulation requires several anthropometric measures as the inputs to the mechanical model of human body dynamics, including moment of inertia of the body about the ankle (I), body mass (M), height of whole-body COM (h), mass of the feet (m_F), height of the ankle (h_F), and anterior–posterior (A/P) distance between the ankle and the COM of the feet (d_F). Several measures were obtained directly from each participant prior to the experimental trials: M, stature (l) and foot length (l_F). The remaining measures were estimated as follows (Qu and Nussbaum, 2009):

$$\begin{cases} I = M \times l^2 \times [0.3^2 + (0.588 - 0.039)^2]; \\ h = l \times (0.588 - 0.039); \\ m_F = M \times 0.0137 \times 2(male) \text{ or } m_F = M \times 0.0129 \times 2(female); \\ h_F = l \times 0.039; \\ d_F = l_F \times 0.4415(male) \text{ or } d_F = l_F \times 0.4014(female). \end{cases} \quad (1)$$

2.2. Alternative model structures

The balance control models presented here and their implementation are modified from our earlier approach (Qu et al., 2007), in which the neural controller is assumed to be an optimal controller that can minimize a performance index defined by physical quantities relevant to sway. Human body dynamics are represented by a single-segment inverted pendulum model (Fig. 1(a)), and sensory systems are assumed to provide accurate body orientation information to the neural controller but with a certain time delay. Experimental data are needed to specify model parameters, such as sensory delay time, and this specification is accomplished using an optimization procedure which adopted heuristic search approaches.

Two model structures were developed here, differing in active/passive control components (Fig. 1(b)). Specifically, the NP (no-passive) model structure accounted only for active control torque, whereas both passive stiffness and damping components were also included in the PA (passive+active) model structure (Maurer and Peterka, 2005). According to active control theories, the active control torque in both model structures is generated from the neural controller and involves a time delay. Passive stiffness and passive damping torques in the PA model structure are proportional to sway angular displacement and its velocity, respectively, without time delay; this approach is consistent with passive control patterns proposed in previous studies (Winter et al., 2001; Maurer and Peterka, 2005).

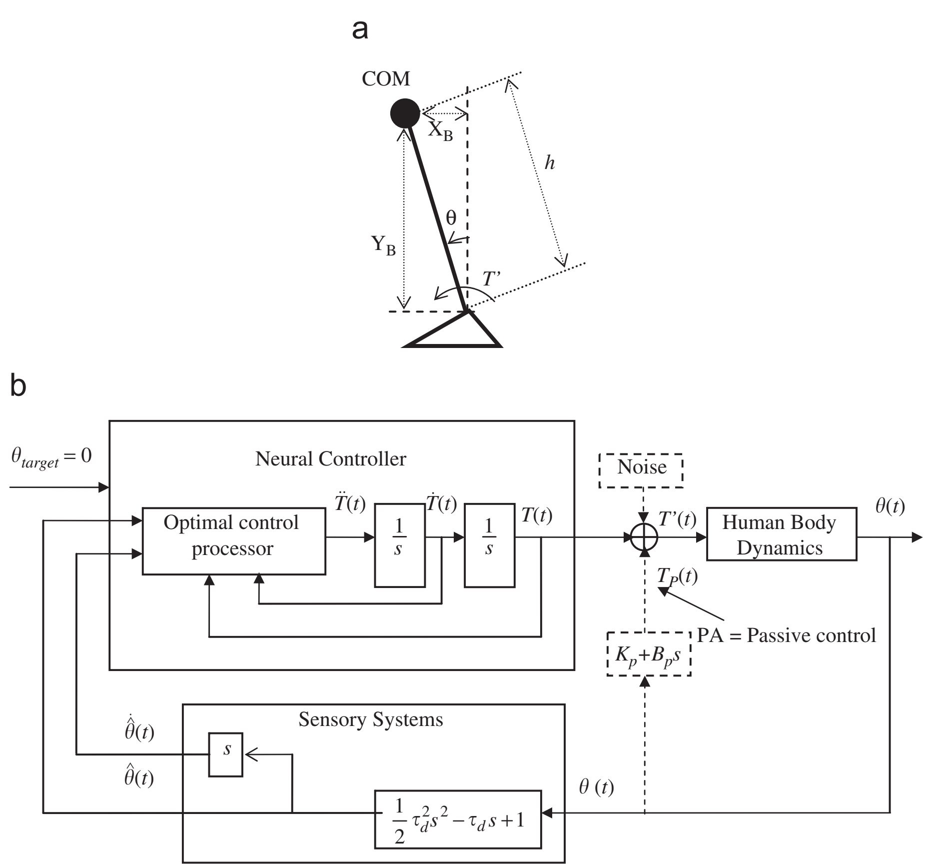

Fig. 1. (a) Inverted pendulum model of human body dynamics; (b) two alternative optimal control model structures used to simulate postural control. Both models included an active control component (the outer feedback loop). The NP (no passive) model included only active control, whereas the PA (passive+active) model also had a passive control component (the dashed inner feedback loop). θ = sway angular displacement; $\hat{\theta}$ = delayed sway angular displacement; T' = ankle torque; T = active control torque generated by the neural controller; θ_{target} = target sway angle; τ_d = sensory delay time; K_P = passive stiffness parameter; B_p = passive damping parameter; T_P = passive control torque.

2.3. Controlled state equations for different model structures

The controlled state equations for the NP model structure (Fig. 1(b)) are as follows (this model is identical to that reported in Qu et al. (2007), to which the reader is referred for additional details):

$$\dot{x}(t) = Ax(t) + Bu(t) \tag{2}$$

where

$$A = \begin{pmatrix} 0 & 1 & 0 & 0 \\ \frac{Mgh}{I} & 0 & \frac{1}{I} & \frac{-\tau_d}{I} \\ 0 & 0 & 0 & 1 \\ 0 & 0 & 0 & 0 \end{pmatrix}, \quad B = \begin{pmatrix} 0 \\ \frac{\tau_d^2}{2I} \\ 0 \\ 1 \end{pmatrix},$$

the state is

$$x(t) = \begin{pmatrix} \hat{\theta}(t) \\ \dot{\hat{\theta}}(t) \\ T(t) \\ \dot{T}(t) \end{pmatrix},$$

the control signal is $u(t) = \ddot{T}(t)$. These state equations account for the properties of body dynamics and sensory systems.

In contrast to the NP model structure, passive control torque is included in the PA model structure (Fig. 1(b)). Therefore, in addition to the properties of body dynamics and sensory systems, intrinsic passive mechanical properties need to be taken into account by the neural controller to stabilize the upright posture. Since the joint torque (T') is the sum of active control torque (T) and passive control torque (T_P), a transfer function from the torque generated by the neural controller (T) to delayed sway angular displacement ($\hat{\theta}$) is given by

$$\frac{\hat{\theta}(s)}{T(s)} = \frac{(1/2)\tau_d^2 s^2 - \tau_d s + 1}{Is^2 + B_p s - (K_p - Mgh)} \tag{3}$$

The Laplace 's' can be replaced by the differentiation operator. Thus, the state equations accounting for intrinsic passive mechanical properties as well as the properties of body dynamics and sensory systems are as follows:

$$\dot{x}(t) = Ax(t) + Bu(t) \tag{4}$$

where

$$A = \begin{pmatrix} 0 & 1 & 0 & 0 \\ \frac{Mgh - K_p}{I} & -\frac{B_p}{I} & \frac{1}{I} & \frac{-\tau_d}{I} \\ 0 & 0 & 0 & 1 \\ 0 & 0 & 0 & 0 \end{pmatrix}, \quad B = \begin{pmatrix} 0 \\ \frac{\tau_d^2}{2I} \\ 0 \\ 1 \end{pmatrix},$$

the state is

$$x(t) = \begin{pmatrix} \hat{\theta}(t) \\ \dot{\hat{\theta}}(t) \\ T(t) \\ \dot{T}(t) \end{pmatrix},$$

and the control signal is $u(t) = \ddot{T}(t)$.

2.4. Optimal control processor and optimization procedure

The optimal control processor (see Fig. 1(b)) is determined by an infinite-time linear quadratic regulator, which minimizes a performance index defined by a weighted combination of several physical quantities relevant to sway (Eq. (5)).

$$J = \frac{1}{2}\int_0^\infty (w_1\hat{\theta}^2(t) + w_2\dot{\hat{\theta}}^2(t) + w_3 T^2(t) + w_4 \dot{T}^2(t) + w_5 \ddot{T}^2(t))\,dt \tag{5}$$

Optimal feedback gains can be obtained according to the state equations of the controlled part (Eqs. (2) or (4)) and used to define the optimal control processor. Some model parameters, such as sensory delay times and passive parameters, cannot be specified before model simulation. Thus, an optimization procedure was performed to determine the values of these unspecified model parameters, using the following cost function:

$$E = \sum_{i=1}^{N} \left(\frac{COPM_i - CO\hat{P}M_i}{CO\hat{P}M_i} \right)^2 \tag{6}$$

where $N = 9$ is the number of COP-based measures, and $COPM_i$ and $CO\hat{P}M_i$ are the ith COP-based measure from the simulation results and from the experimental results, respectively. The nine COP-based measures used to define the cost function were selected according to the classification suggested by Maurer and Peterka (2005), with additional details provided in Qu et al. (2007). Heuristic approaches (i.e., a genetic algorithm (GA) and simulated annealing (SA)) were implemented to determine model parameters (Hillier and Lieberman, 2005).

2.5. Dependent COP-based measures

Performance of the two balance control model structures was evaluated by their ability to simulate several measures derived from COP time series, which have been commonly used to characterize postural sway behaviors. In general, COP-based measures can be classified as 'traditional' measures and those derived from statistical mechanics (Norris et al., 2005; Collins and De Luca, 1993). In this study, four traditional and four statistical mechanics COP-based measures were selected as dependent measures (Qu and Nussbaum, 2009). The selected traditional measures (root mean squared distance (RMS), mean velocity (MV), centroidal frequency (CFREQ), frequency dispersion (FREQD)) account for both time-domain and frequency-domain properties of COP time series. The dependent statistical mechanics measures (transition time (TT), transition amplitude (TA), short-term scaling exponent (H_S), and long-term scaling exponent (H_L)) were based on a fractional Brownian motion (fBm) model (Rougier, 1999). Specifically, the transition point, which is critical to determine these selected statistical mechanics measures, was found from the largest vertical distance between the logarithm of the diffusion curve and the theoretical straight line (Rougier, 1999).

2.6. Model simulation and analysis

The two proposed model structures were separately used to simulate the 48 experimental trials (16 participants $\times$ 3 trials/participant). Each simulation trial was 75 s in duration, with the initial 10 s and last 5 s removed to be consistent with the experimental data. Simulated and experimental COP-based measures were compared using two-sample t-tests to examine the extent to which the alternative model structures could accurately simulate COP time series.

To quantify simulation performance, scalar errors (e) between simulated and experimental data were determined for each dependent COP-based measure:

$$e = \left| \frac{m_{sim} - m_{ref}}{m_{ref}} \right| \tag{7}$$

where m_{sim} is a simulated dependent COP-based measure for a given simulation trial, and m_{ref} is the corresponding experimental measure. Separate comparison of scalar errors between model structures was performed for each dependent COP-based measure using two-sample t-tests. For all statistical tests, the level of significance (α) was set at 0.05. In addition, from the simulation results using the PA model structure, ratios between the mean amplitudes of absolute passive and active control torques were calculated for each simulation trial. The distribution of these ratios was analyzed to identify the relative importance of passive and active control torques in balance control.

3. Results

There were no significant differences between simulated and experimental data for most of the dependent COP-based measures (Table 1). Exceptions occurred in TT and TA using both model structures. Specifically, mean (SD) values of simulated TT and TA using the NP model structure were 1.092 (0.372) s and 33.9 (22.6) mm^2, respectively, which were both significantly (TT: $p = 0.002$; TA: $p = 0.024$) larger than experimental values of TT ($= 0.658$ (0.427) s) and TA ($= 20.4$ (12.9) mm^2). The PA model structure also generated significantly larger TT ($= 1.226$ (0.133) s) and TA ($= 31.5$ (18.7) mm^2) when compared with experimental data ($p < 0.001$ and $p = 0.031$, respectively). Both model structures yielded RMS and MV measures comparable to those observed experimentally. Though not significant ($p = 0.08$), both structures yielded CFREQ and FREQD magnitudes that were typically higher and lower, respectively, than was measured. Both models also tended to predict scaling exponents (H_S and H_L) that were smaller than observed, though the NP-simulated values exhibited less of a discrepancy.

Scalar errors (i.e., between simulated and experimental dependent COP-based measures) were diverse across the different measures (Table 2). For all measures, average scalar errors generated from the NP model structure were smaller than those

Table 1
Comparisons between simulated and experimental dependent COP-based measures: Mean (SD).

	NP			PA		
	Simulated	Experimental	*p*-Value	Simulated	Experimental	*p*-Value
RMS	5.76 (1.98)	5.85 (2.03)	0.451	5.72 (1.93)	5.85 (2.03)	0.428
MV	9.17 (2.50)	8.70 (2.35)	0.294	9.30 (2.50)	8.70 (2.35)	0.246
CFREQ	0.492 (0.087)	0.548 (0.126)	0.080	0.502 (0.062)	0.548 (0.126)	0.098
FREQD	0.929 (0.021)	0.913 (0.040)	0.078	0.929 (0.023)	0.913 (0.040)	0.083
TT	1.092 (0.372)	0.658 (0.427)	0.002	1.226 (0.133)	0.658 (0.427)	<0.001
TA	33.9 (22.6)	20.4 (12.9)	0.024	31.5 (18.7)	20.4 (12.9)	0.031
H_S	0.780 (0.029)	0.795 (0.052)	0.167	0.767 (0.058)	0.795 (0.052)	0.082
H_L	0.187 (0.114)	0.222 (0.096)	0.178	0.171 (0.108)	0.222 (0.096)	0.087

Table 2
Scalar errors (Mean (SD)) between simulated and experimental dependent COP-based measures.

COP-based measure	NP	PA	*p*-Value
RMS	0.0228 (0.0221)	0.0312 (0.0188)	0.023
MV	0.0626 (0.0445)	0.0760 (0.0401)	0.062
CFREQ	0.143 (0.173)	0.147 (0.170)	0.458
FREQD	0.0391 (0.0318)	0.0413 (0.0327)	0.368
TT	1.13 (0.624)	1.17 (0.578)	0.413
TA	0.958 (0.817)	0.996 (0.989)	0.419
H_S	0.0718 (0.0660)	0.0993 (0.0756)	0.030
H_L	0.453 (0.319)	0.532 (0.311)	0.111

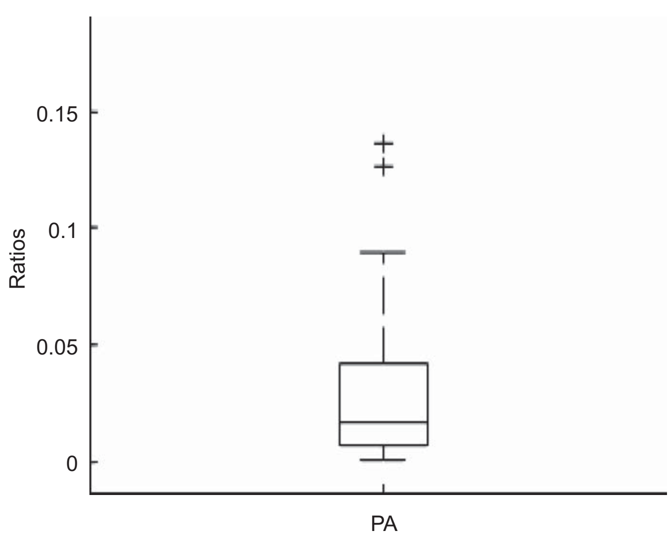

Fig. 2. Box plot of ratios between the means of absolute passive and active control torques from the PA model structure. Horizontal lines in the box represent the lower quartile, median, and upper quartile. Whiskers indicate 1.5 times the interquartile range, and '+' symbols identify outliers beyond the whiskers.

from the PA model. These differences were significant for scalar errors in RMS and H_S, and approached significance for MV. As a ratio, scalar errors from the NP model were 72.3–97.3% of those from the PA model.

In the PA model structure, passive joint torque generated by passive tissues was considered, and the mean ratio of passive to active control torques was 0.034. From the distribution of this ratio (Fig. 2), some outliers were likely present; disregarding these outliers, the maximum ratio was only the order of 0.090. Predicted

Table 3
Predicted passive stiffness (K_P) and passive damping (B_P) using the PA model structure.

Participant #	Passive stiffness (Nm/rad)	Passive damping (Nm s/rad)
1	13.69	6.47
2	14.17	2.74
3	6.45	4.11
4	20.58	3.86
5	7.07	2.66
6	17.88	1.30
7	4.61	3.75
8	14.67	7.12
9	58.44	1.56
10	19.04	4.77
11	18.66	4.51
12	12.81	10.19
13	9.59	3.16
14	28.89	5.22
15	12.22	2.48
16	16.52	25.63

passive stiffness (K_P) was in the range of 4.6–58.4 Nm/rad across participants. Minimum and maximum values of passive damping (B_P) were 1.3 and 25.6 Nm s/rad, respectively (Table 3).

4. Discussion

According to current balance control theories, which differ in terms of the roles of passive and active mechanisms in balance control, two model structures were developed, evaluated, and used to provide new information regarding these roles. The simulation results from both model structures showed that most of the simulated dependent COP-based measures were not significantly different from their corresponding experimental measures (Table 1), indicating that these models appear to be capable of accurately simulating postural sway behaviors characterized by COP time series. Thus, these models should be useful for examining alternative balance control theories, such as the contribution of passive control here.

Scalar errors between simulated and experimental data were obtained for each dependent COP-based measure, and used to quantify the performance of both model structures. Ideally, these scalar errors would be zero, indicating an exact model duplication (or simulation) of the experimental data. Based on actual scalar errors obtained (Table 2), the NP model structure was superior at simulating RMS and H_S. In addition, the remaining scalar errors were all smaller in the NP model structure as well. Since this set of measures derived from COP time series should reflect the major underlying characteristics of postural sway behaviors, it can be concluded that the NP model structure simulated balance control better than the PA structure. Since the PA model structure accounted for passive control, yet including passive control did not improve the model's performance, it would appear from this that passive control does not make a substantial contribution to maintaining upright balance.

That the NP model structure performed better in terms of simulating COP does not, however, necessarily refute the existence of passive components in balance control. Here, an optimization procedure using both a GA and SA was to identify an 'optimal' set of model parameters. Both the GA and SA are heuristic methods and are not guaranteed to find global optima. The PA model structure had two additional free model parameters (i.e., K_P and B_P), and thus involved a more complex optimization problem. As such, the heuristic search may have been relatively less effective, and might explain the somewhat counterintuitive result that the NP model structure performed better. Nonetheless, there still would seem support for the conclusion that passive control does not play an important role in the control of balance.

Using the PA model, the maximum ratio (disregarding outliers) of passive to active control torques was approximately 0.090 (Fig. 2). This provides additional evidence that active control torques are an order of magnitude more important than passive control torques in maintaining upright balance. Similar results were reported by Peterka (2002), who applied a PID neural controller to simulate balance control; passive stiffness and damping parameters obtained from their simulation were found to be only $\frac{1}{10}$ the value of active stiffness and damping parameters. In addition, the critical stiffness, which is the minimal necessary to achieve stability without an active stabilization mechanism, is typically over 300 Nm/rad (Casadio et al., 2005). However, the values of predicted passive stiffness here were on the order of 4.6–58.4 Nm/rad (Table 3), far smaller than the critical stiffness and clearly insufficient as a sole mechanism to maintain upright stability. Based on these and the results from scalar errors, our hypothesis appeared to be supported: that active control torque plays a substantially more important role in balance control than does passive control torque.

Some existing studies (e.g., Casadio et al., 2005; Loram and Lakie, 2002b) have experimentally quantified passive ankle stiffness to evaluate the patterns of active and passive components in balance control. Experimental studies may be limited by the available experimental methods and equipment, and thus may not provide sufficient insights into internal balance control mechanisms. Mathematical models can be a good complement to experimental studies, and can predict internal balance control mechanisms based on reasonable assumptions. Thus, this study investigated the roles of passive and active control torques in balance control from a different perspective versus existing experimental studies.

Mathematical models have also been used to investigate passive/active control of balance in other studies (e.g., Peterka, 2002; Winter et al., 1998). Peterka (2002) developed a PID (proportional, derivative, and integral) balance control model, and used this model to estimate passive and active stiffness. However, the ability of their model to simulate COP was not presented. In contrast, the performance of the current NP and PA model structures was formally assessed in terms of their ability to simulate COP-based measures. Such measures are commonly used in balance control studies since COP time series are in phase with COM time series, and reflect the net motor control signal output necessary to keep the projection of the COM within the base of support (Cavanaugh et al., 2005; Prieto et al., 1993). Thus, model-based simulation here provides a new way to examine divergent balance control theories.

Experimental values of traditional measures were used as references to calculate the cost function (Eq. (6)) during simulation. In contrast, experimental values of the statistical mechanics measures were only used during post-simulation evaluations of model performance. Thus, it seems unlikely that simulated traditional measures and simulated statistical mechanics measures would have the same level of accuracy. This argument may help explain why the scalar errors of the statistical mechanics measures were typically larger than those of the traditional measures (Table 2). In addition, simulated TT and TA were found to be significantly larger than their experimental references, suggesting that the simulated postural control system adopts a longer and larger open-loop control scheme than the actual one. This latter discrepancy likely occurred because the single-segment inverted pendulum body model can only provide limited feedback (closed-loop) information (i.e., ankle angular displacement) to the model neural controller.

There were important potential limitations in this study that should be noted. First, some anthropometric measures were estimated, and thereby served as a source of errors in the model simulation. Since comparisons between model structures were made 'within-subjects', such errors are not expected to have confounded the primary conclusions. Second, limitations and assumption exist within the fundamental approach and framework used (see Qu et al. (2007) for a more complete discussion). For example, the assumption that the neural controller adopts an optimal control strategy has not been validated. However, diverse evidence supports the role of optimality in motor and postural control (e.g., Ohta et al., 2004; Fagg et al., 2002). Thus, this assumption is expected to be reasonable. Finally, the present results only account for attributes of balance control in the A/P direction (sagittal plane). In future research, three-dimensional balance control model structures should be investigated.

In summary, the relative contributions of active and passive control during quiet upright stance were investigated by implementing alternative balance control model structures. Results based on model performance (i.e., accuracy of simulation) and simulated magnitudes of active and passive torques both suggest that active control torque is predominant in maintaining upright balance, which supports the initial hypothesis. Support was also provided for the utility of such mathematical models to examine the validity of different balance control theories.

Conflict of interest

The authors declare that both authors have no financial or personal relationship with other persons or organizations that might inappropriately influence our work presented therein.

Acknowledgement

This work was supported in part by Cooperative Agreement Number R01 OH0078802 from the Centers for Disease Control and Prevention (CDC) and by a Start-up Grant (WBS Element M58050017) from Nanyang Technological University (NTU). Its contents are solely the responsibility of the authors and do not necessarily represent the official views of CDC or NTU.

References

Applegate, C., Gandevia, S.C., Burke, D., 1988. Changes in muscle and cutaneous cerebral potentials during standing. Experimental Brain Research 71, 183–188.
Casadio, M., Morasso, P.G., Sanguineti, V., 2005. Direct measurement of ankle stiffness during quiet standing: implications for control modeling and clinical application. Gait & Posture 21, 410–424.

Cavanaugh, J.T., Guskiewicz, K.M., Stergiou, N., 2005. A nonlinear dynamic approach for evaluating postural control. Sports Medicine 35, 935–950.
Collins, J.J., De Luca, C.J., 1993. Open loop and closed loop control of posture: a random-walk analysis of center of pressure trajectories. Experimental Brain Research 95, 308–318.
Fagg, A.H., Shah, A., Barto, A.G., 2002. A computational model of muscle recruitment for wrist movement. Journal of Neurophysiology 88, 3348–3358.
Hillier, E.S., Lieberman, G.J., 2005. Introduction to Operations Research. McGraw Hill, New York.
Lakie, M., Caplan, N., Loram, I.D., 2003. Human balancing of an inverted pendulum with a compliant linkage: neural control by anticipatory intermittent bias. Journal of Physiology 551, 357–370.
Loram, I.D., Lakie, M., 2002a. Direct measurement of human ankle stiffness during quiet standing: the intrinsic mechanical stiffness is insufficient for stability. Journal of Physiology 545, 1041–1053.
Loram, I.D., Lakie, M., 2002b. Human balancing of an inverted pendulum: position control by small, ballistic-like, throw and catch movements. Journal of Physiology 540, 1111–1124.
Masani, K., Vetter, A.H., Popovic, M.R., 2006. Controlling balance during quiet standing: proportional and derivative controller generates preceding motor command to body sway position observed in experiments. Gait & Posture 23, 164–172.
Maurer, C., Peterka, R.J., 2005. A new interpretation of spontaneous sway measures based on a simple model of human postural control. Journal of Neurophysiology 93, 189–200.
Morasso, P.G., Schieppati, M., 1999. Can muscle stiffness alone stabilize upright standing?. Journal of Neurophysiology 83, 1622–1626.
Morasso, P.G., Sanguineti, V., 2002. Ankle muscle stiffness alone cannot stabilize balance during quiet standing. Journal of Neurophysiology 88, 2157–2162.
Norris, J.A., Marsh, A.P., Smith, I.J., Kohut, R.I., Miller, M.E., 2005. Ability of static and statistical mechanics posturographic measures to distinguish between age and fall risk. Journal of Biomechanics 38, 1263–1272.
Ohta, K., Svinin, M.M., Luo, Z., Hosoe, S., Laboissiére, R., 2004. Optimal trajectory formation of constrained human arm reaching movements. Biological Cybernetics 91, 23–36.
Peterka, R.J., 2002. Sensorimotor integration in human postural control. Journal of Neurophysiology 88, 1097–1118.
Prieto, T.E., Myklebust, J.B., Hoffmann, R.G., Myklebust, B.M., 1993. Characterization and modeling of postural steadiness in the elderly: a review. IEEE Transactions on Rehabilitation Engineering 1, 26–34.
Qu, X., Nussbaum, M.A., 2009. Effects of external loads on balance control during upright stance: experimental results and model-based predictions. Gait & Posture 29, 23–30.
Qu, X., Nussbaum, M.A., Madigan, M.L., 2007. A balance control model of quiet upright stance based on an optimal control strategy. Journal of Biomechanics 40, 3590–3597.
Rougier, P., 1999. Influence of visual feedback on successive control mechanisms in upright quiet stance in humans assessed by fractional Brownian motion modeling. Neuroscience Letters 266, 157–160.
Winter, D.A., Patla, A.E., Prince, F., Ishac, M., 1998. Stiffness control of balance in quiet standing. Journal of Neurophysiology 80, 1211–1221.
Winter, D.A., Patla, A.E., Prince, F., Ishac, M., 2001. Ankle muscle stiffness in the control of balance during quiet standing. Journal of Neurophysiology 85, 2630–2633.
Winter, D.A., Patla, A.E., Ishac, M., Gage, W.H., 2003. Motor mechanisms of balance during quiet standing. Journal of Electromyography and Kinesiology 13, 49–56.